ELSEVIER

Chemical Engineering Journal 140 (2008) 432–438

Chemical Engineering Journal

www.elsevier.com/locate/cej

# Carbonaceous materials as catalysts for decomposition of methane

I. Suelves *, J.L. Pinilla, M.J. Lázaro, R. Moliner

*Instituto de Carboquímica CSIC, Miguel Luesma Castán 4, 50015 Zaragoz, Spain*

Received 10 July 2007; received in revised form 5 November 2007; accepted 9 November 2007

**Abstract**

Thermo-catalytic decomposition of methane over different carbonaceous materials was studied by monitoring the mass gain with time. The initial decomposition rates as well as the long-term behaviour of the catalyst (i.e. the carbon mass that the catalyst can accumulate before deactivation occurs) were determined for a wide range of carbon blacks (CB) with different textural properties and surface chemistry, and for a commercial activated carbon (AC). The commercial carbon black BP2000 showed the highest amount of carbon deposited, 6.13 g $C_{dep}$/g $C_o$ before deactivation while the higher initial carbon formation rate ($r_o$) among the different samples tested was obtained for the activated carbon CG Norit (85.9 mg $C_{dep}$/g $C_o$ min). The relationship between the characteristics of the carbonaceous materials and their efficiency as catalysts were also evaluated. The amount of carbon deposited until deactivation shows a linear relationship with the total pore volume of the fresh catalysts. A good correlation is also found between the initial reaction rate and the concentration of oxygenated groups desorbed as CO after a temperature-programmed desorption (TPD) experiment.


*Keywords:* Hydrogen production; Methane decarbonization; Carbon catalysts

## 1. Introduction

Thermo-catalytic decomposition, TCD, of natural gas, with carbon being captured as a solid of added value product, appears as an interesting alternative to steam reforming for hydrogen production [1–5]. Two different nature catalysts have been used for this process: metallic and carbonaceous catalysts [6–9]. Carbon catalysts were proposed as an alternative to metallic catalysts [10–16] because they offer several advantages: (i) higher fuel flexibility and no sulphur poisoning; (ii) lower price; (iii) the carbon formed can be used as catalyst precursor, so that the process is self-sustained.

TCD of methane using carbonaceous catalysts was studied extensively by our research group using a bench scale fixed bed reactor designed for studying carbonaceous materials of different origin/nature [13–15]. In a second step, the kinetic parameters for two selected commercial carbonaceous materials, an activated carbon (CG Norit) and a carbon black (BP2000), were obtained using a thermobalance to monitor the mass gain with time [16]. This method overcomes the plugging problems that occur when fixed bed reactors are used [17,18]. This method has been widely used to study the TCD of methane when metal catalysts were used [19–22], but no references have been found related to the use of carbon catalysts. We reported [16] that the methane decomposition over carbonaceous catalysts was a half-order reaction, and the activation energies were 141 kJ/mol and 238 kJ/mol, for the activated carbon and the carbon black, respectively.

In present work using the thermobalance, the initial decomposition rates as well as the long-term behaviour of the catalysts (that is, the carbon mass that the catalyst can accumulate before deactivation occurs), have been determined for a wide range of carbon blacks (CB) with different textural properties and surface chemistry. The findings are also reported for a commercial activated carbon (AC) used in our previous works at bench scale. The AC showed an acceptable initial reaction rate but became rapidly deactivated, while the CB with a high surface area provided more stable and sustainable hydrogen production.

Besides this, the fresh catalysts have been characterized by measuring their textural properties and surface chemistry, as well as their crystallinity and morphology. This was done in order to study the relationship between the characteristics of the carbonaceous materials and their efficiency as catalysts in more detail.

* Corresponding author. Tel.: +34 976733977; fax: +34 976733318.
*E-mail address:* isuelves@icb.csic.es (I. Suelves).

1385-8947/$ – see front matter © 2007 Elsevier B.V. All rights reserved.
doi:10.1016/j.cej.2007.11.014

Table 1
Proximate and ultimate analysis of the samples

| | C | H | N | S | O[a] | Moisture | Ash | Volatile matter |
|---|---|---|---|---|---|---|---|---|
| CG Norit | 70.2 | 2.87 | 0.13 | 0 | 26.76 | 9.78 | 2.77 | 11.74 |
| Fluka 05120 | 86.7 | 0.29 | 0.58 | 0.55 | 12.41 | 2.66 | 6.34 | 1.95 |
| XC72 | 99.2 | 0.12 | 0.15 | 0.61 | 0.54 | 0.26 | 0.04 | 0.8 |
| BP1300 | 83.7 | 0.52 | 0.37 | 0.8 | 15.41 | 6.94 | 1.89 | 10.11 |
| BP2000 | 97.1 | 0.2 | 0.16 | 0.73 | 2.56 | 0.5 | 1.02 | 1.65 |
| BP1100 | 94.7 | 0.2 | 0.32 | 0.82 | 4 | 1.51 | 1.61 | 4.16 |

[a] Calculated by difference.

## 2. Experimental

### 2.1. Samples

Five different commercial carbon black samples, XC72, BP1100, BP1300, BP2000 (Cabot), Fluka 05120, and a commercial active carbon (CG Norit) were used as catalysts for the TCD of methane. Table 1 shows the ultimate and proximate analysis of the samples. The CG Norit sample presents the highest oxygen content.

### 2.2. Experimental set-up

Methane decomposition experiments were conducted in a Cahn TG 151 Thermogravimetric Analyzer. This experimental set-up allows for continuous recording of sample weight changes and temperature during reaction. At atmospheric pressure, the thermobalance can operate up to 1000 °C. The thermobalance consists of three main sections: the hardware (pressure balance, furnace, stand), the software (electronic components and display) and the external flow, pressure and temperature controllers. An internal quartz tube sealed at both ends with O-rings separates the reactor chamber from the furnace. The loading and unloading of the sample is accomplished by opening the joint and lowering the furnace with the help of an automatic elevator. The temperature inside the reactor chamber is measured and controlled by a 1/8 in. Chromel–Alumel thermocouple located just below the sample holder. The sample holder is a quartz basket (14 mm diameter and 8 mm height) to reduce mass transfer resistance around the solid sample. Operating conditions were: carbon weight 30 mg, methane flow rate: 3 l/h.

The samples released tar and water during the first stage of the runs. In order to stabilize the catalyst, they were pretreated under nitrogen at the reaction temperature before the reaction tests until a constant weight was reached. The desired temperature was reached using a heating rate of 20 °C/min.

### 2.3. Characterization techniques

The textural properties of the fresh samples were measured by $N_2$ adsorption at 77 K in a Micromeritics ASAP2020 apparatus. The specific surface was calculated by applying the BET method to the $N_2$ adsorption isotherms. The total pore volume of the samples was measured by Hg porosimetry in a Pore Master Quantachrome apparatus.

The amount of CO and $CO_2$ released was determined by temperature-programmed desorption (TPD). First, the profiles of released CO and $CO_2$ were obtained in a fixed bed reactor heated under a constant flow of He (30 ml/min) at a heating rate of 10 °C/min (up to a temperature of 1050 °C). The eluted gas was collected in separated gas sampling bags corresponding to consecutive temperature ranges of 100 °C and analyzed by gas chromatography. The total amount of CO and $CO_2$ released was calculated by integrating the area under of the concentration curve versus volume.

Powder X-ray diffraction (XRD) patterns for the study of the crystalline chemical species in both fresh and used catalysts were obtained using a Bruker AXS D8 Advance apparatus.

The morphological appearance of the fresh catalyst and the deposited carbon has been studied by scanning electron microscopy (SEM). The samples analyzed were embedded in an epoxy resin, cut into slides and polished with diamond paste to an optical finish. This was done in order to observe the cross-sectional area of the particle samples before and after TCD reaction.

## 3. Results and discussion

### 3.1. Activity tests

In previous work [16], we stated that during TCD of methane, the maximum amount of carbon that the carbon catalyst can accumulate before deactivation is not dependant on the temperature reaction. This is unlike what happened when metal catalysts were used, which are very sensitive to the operation conditions [23]. However, the kinetic constants are increased with an increase in the reaction temperature, which provokes an enhancement in the reaction rate. The thermobalance runs were carried out in isothermal conditions (900 °C) for all the catalysts tested. As we have previously mentioned, the thermobalance allows us to measure directly the weight changes as the methane is decomposed and the carbon is deposited into the carbon samples. Table 2 summarizes the most important parameters extracted from the activity runs carried out at 900 °C in the thermobalance: maximum amount of carbon deposited per initial catalyst mass before deactivation $(C_{dep}/C_o)_{deact}$ and initial reaction rate ($r_o$). Fig. 1 shows the change of the carbon deposited with time, expressed as the mass ratio of the deposited carbon to the initial carbon catalyst ($C_{dep}/C_o$), for the BP2000 and XC72 samples (Fig. 1a) and for the BP1100, BP1300, Fluka

Table 2
Features of the carbonaceous samples used in thermobalance run at 900 °C

| | $(C_{dep}/C_o)_{deact}$ | $r_o$ (mg $C_{dep}$/g $C_o$ min) |
|---|---|---|
| CG Norit | 0.70 | 85.9 |
| Fluka05120 | 0.49 | 17.8 |
| XC72 | 2.74 | 6.4 |
| BP1300 | 1.45 | 24.5 |
| BP2000 | 6.13 | 9.4 |
| BP1100 | 0.78 | 15.5 |

05120 and CG Norit samples (Fig. 1b) tested at 900 °C. The runs were carried out in the thermobalance until the mass gain was almost negligible. It was observed that the commercial carbon black BP2000 shows the highest amount of carbon deposited (it can accumulate 6.13 g $C_{dep}$/g $C_o$). For the other samples tested, the amount of carbon deposited was lower, ranging from 1.4 to 2.7 g $C_{dep}$/g $C_o$ when BP1300 and XC72 were used, to 0.5–0.7 when BP1100, Fluka and CG Norit were used.

Fig. 2 shows the evolution of the carbon formation rate, expressed as mg $C_{dep}$/g $C_o$ min, for the BP2000 and XC72 samples (Fig. 2a) and for the BP1100, BP1300, Fluka 05120 and CG Norit samples (Fig. 2b). The evolution of the formation rate

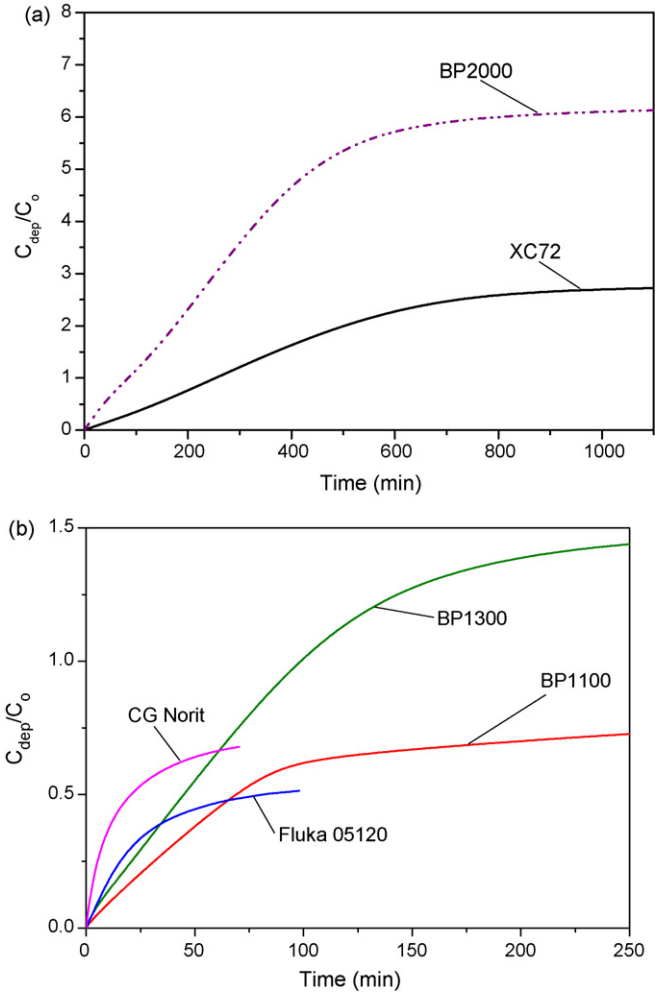


Fig. 1. (a and b) Evolution with time of the carbon deposited for different carbon catalysts. Reaction temperature: 900 °C.

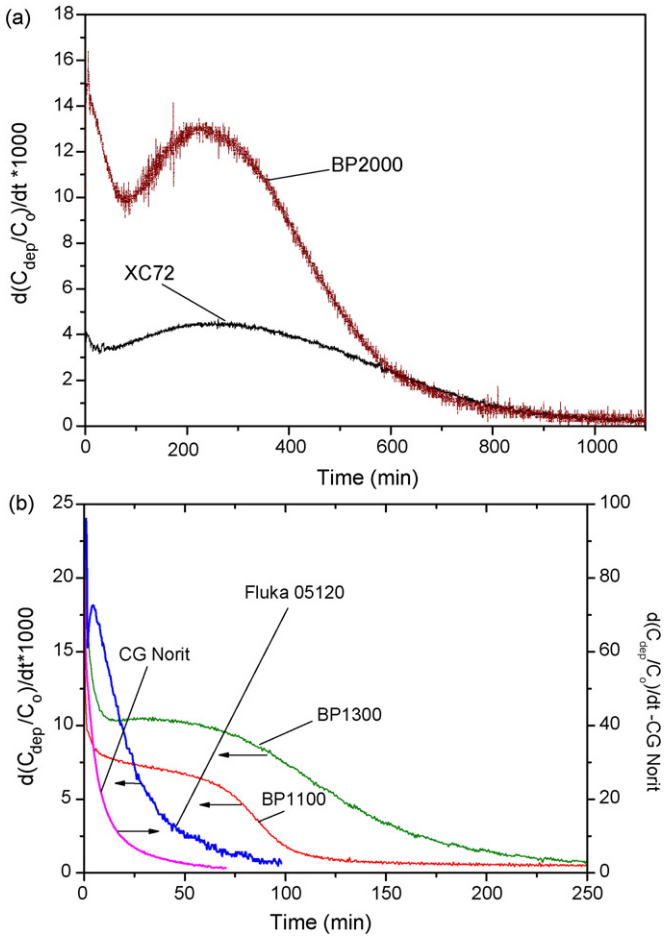


Fig. 2. (a and b) Evolution of the carbon formation rate along time $r_c$ (g carbon/g cat min) versus time (min) for different carbon catalysts. Reaction temperature: 900 °C.

was calculated from the derivative of the data plotted in Fig. 1. The highest initial carbon formation rate ($r_o$) among the different samples tested was obtained from the activated carbon CG Norit (85.9 mg $C_{dep}$/g $C_o$ min), but this high rate was followed by a rapid deactivation, following an exponential decay. The carbon black samples tested presented lower $r_o$, ranging from 6.4 for the XC72 to 24.5 for the BP1300. These samples present a different trend in comparison to the activated carbon: at the beginning of the run a relative high initial carbon formation rate was observed. For the Fluka 05120, XC72 and BP2000 samples, the $r_o$ then increased until a maximum was reached. Meanwhile, for the BP1100 and BP1300, a steady state was observed, followed in all cases by a progressive decline in the reaction rate for all the samples until negligible values of mass gained were obtained.

In previous work, we stated a possible explanation for the form of the kinetic curve of the BP2000 sample [16], which can also be extended to all the carbon black samples used in the present work. The curves can be divided into three main zones. Zone (1) corresponds to the exponential decay in the reaction rate: this decay may be due to the decrease in the surface oxygenated groups. It has been previously reported [13–15] that the oxygen surface groups play a key role in the initial reaction

Table 3
Surface chemistry and textural properties of the fresh carbonaceous samples

| | $S_{BET}$ ($m^2$/g) | $V_p$ ($cm^3$/g) | CO ($cm^3$/g) | $CO_2$ ($cm^3$/g) |
|---|---|---|---|---|
| CG Norit | 1300 | 0.947 | 28.13 | 3.98 |
| Fluka05120 | 788 | 0.74 | 4.97 | 0.02 |
| XC72 | 223 | 1.49 | 6.51 | 0.30 |
| BP1100 | 251 | 0.70 | 7.87 | 6.57 |
| BP1300 | 495 | 0.71 | 13.82 | 9.84 |
| BP2000 | 1337 | 3.06 | 8.23 | 3.75 |

rate. Evidence for the importance of the surface oxygen groups is given below. Zone (2) reflects a pseudo steady state, which is governed by the activity of the crystallites produced from methane. This would correspond to the time in which the original surface area is covered by the carbon crystallites produced from methane, and thus the maximum of the reaction rate due to the crystallites growth is obtained. Zone (3) shows an exponential decay due to the lack of surface area/pore volume where the carbon crystallite could be decomposed.

For the Fluka 05120, BP2000 and XC72 samples in the pseudo steady state, the increase in the rate of methane decomposition due to the increase in the amount of crystallites from methane decomposition is balanced by the decrease in the rate of methane decomposition of the original carbon black sample. This explains the maximum of the kinetic curve. However, for BP1100 and BP1300, this maximum is not present and a shoulder appears.

### 3.2. Relationship between the catalysts performance and their properties

The performance of carbon materials as catalysts is determined by both their texture and surface chemistry [24]. Thus, the textural properties (determined from $N_2$ adsorption at 77 K and Hg porosimetry), and the surface chemistry (determined from the groups desorbed as CO and $CO_2$ in TPD experiments of the fresh samples) have been studied.

#### 3.2.1. Textural properties

Table 3 shows the textural properties (BET area and pore volume) and surface chemistry of the fresh carbon catalyst samples tested in the TCD of methane. In previous work, a good correlation was observed between the amount of carbon accumulated and the BET surface area when different AC were tested in a fixed bed reactor during an 8 h run [13]. In particular, the pore size distribution (especially the mesopore area) was a key factor in defining the long-term behaviour of the catalyst. On the contrary, when different nature carbon samples were studied using a bench scale fixed bed reactor [14], we observed that similar surface areas do not necessarily imply similar carbon deposition. In general, it is accepted that the surface area decreases with the reaction time [25–28], owing to pore blocking by carbon deposition. All of these relationships have to be considered very carefully when carbon catalysts of different natures/families are compared. In the present work, the textural properties of the samples tested in the TCD of methane are related to the total

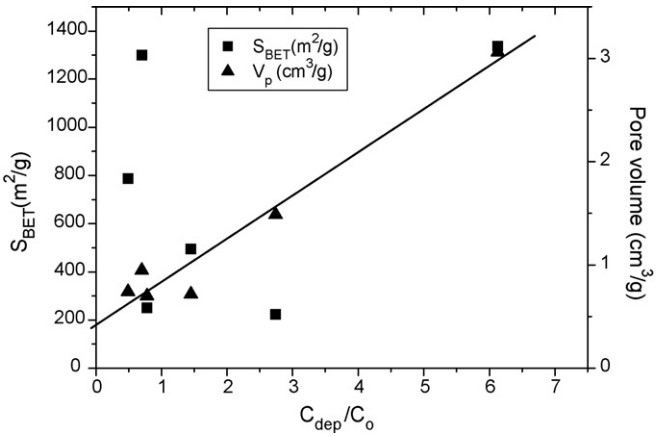


Fig. 3. Carbon deposited per initial catalyst mass for the runs carried out at 900 °C until deactivation versus surface area (left axis) and versus total pore volume (right axis) of the fresh catalyst.

mass of carbon that the carbonaceous samples can accumulate before deactivation occurs, whatever the time needed for the deactivation.

Fig. 3 shows the carbon deposited per initial catalyst mass until deactivation (that is, the long-term efficiency of the catalyst), versus both surface area (left axis) and pore volume (right axis). For example, BP2000 and CG Norit show similar surface areas, but the amount of carbon deposited differs by an order of magnitude. However, when carbon deposited per initial catalyst mass until deactivation is plotted versus total pore volume, a linear relationship is observed.

An estimation of the maximum carbon yield that each material can accommodate can be performed, following the ideal internal diffusion model [29]: this model is based on the assumption that carbon is deposited exclusively inside the particle so that there is no change in starting volume of the granules. On the contrary, in the ideal external diffusion model, the carbon is deposited exclusively on the outer surface of the support grains.

It is known that the theoretical density for graphite is 2.26 cc/g, although most graphite materials will have a lower density due to the presence of structural imperfections such as porosity, lattice vacancies and dislocations [30]. From the pore volume total data, we have calculated the theoretical amount of carbon supposed as graphite that the carbon catalysts are able to accumulate. Fig. 4 shows that a good correlation exists between both parameters, which confirms the important role that the total pore volume plays in the long-term behaviour of the catalyst. The fact that all the points lay over the curve that represent the ideal filling model, highlights that only a fraction of the volume is filled by carbon from the methane decomposition. This could be attributed to blockage of the narrower pores, which hinder the methane diffusion to the active surface of the carbonaceous sample and reduce the effective pore volume in which the carbon can be deposited.

#### 3.2.2. Surface chemistry

TPD has become one of the most outstanding techniques for the evaluation of the surface chemistry in carbon materials [31]. In previous studies, we reported [13,15] the relationship that

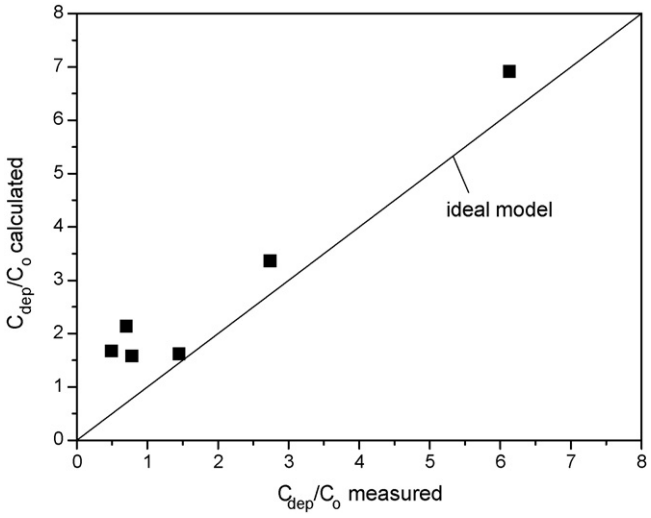


Fig. 4. $C_{dep}/C_o$ calculated versus $C_{dep}/C_o$ measured assuming that the total pore volume is occupied by graphite ($d = 2.26$ cc/g).

exists between the amount of oxygenated surface groups (OSG) desorbed as CO and $CO_2$ after a TPD experiment and the initial activity rate for the fresh catalysts. However, the role and the nature of these oxygenated groups are not yet well understood.

In this work, a more accurate correlation has been found when comparing the OSG desorbed as CO and $CO_2$ from the carbon material after treatment under $N_2$ at 850 °C. As mentioned in Section 2, the carbonaceous catalyst samples released water and tar during the first stage of the runs. This way, no interference with the more labile OSG (which should not affect the catalyst's activities because that they are desorbed during the heating step) is assured. Table 3 shows the amount of CO and $CO_2$ released during TPD runs calculated from the integration of the areas under the curves. Fig. 5 shows the initial conversion rate of the catalysts as a function of the concentration of oxygenated groups: groups desorbed as CO (left axis) and groups desorbed as $CO_2$ (right axis). It can be observed that a good correlation exists between the amount of CO desorbed and the initial reaction rate. The CG Norit presents a high number of groups desorbed as CO,

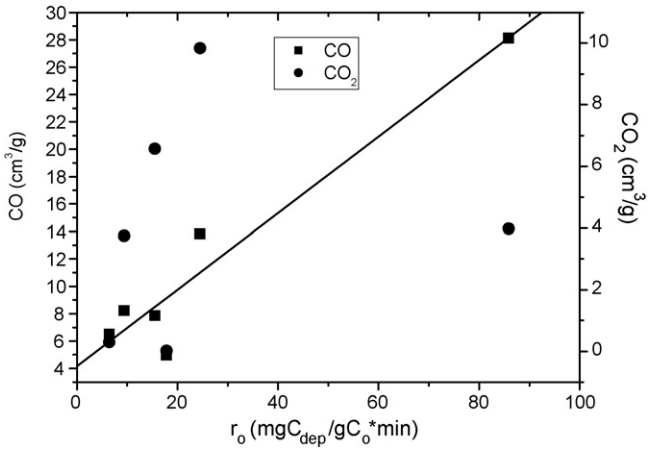


Fig. 5. Initial decomposition rate versus amount of surface oxygenated groups desorbed in TPD runs as CO (left axis) and $CO_2$ (right axis).

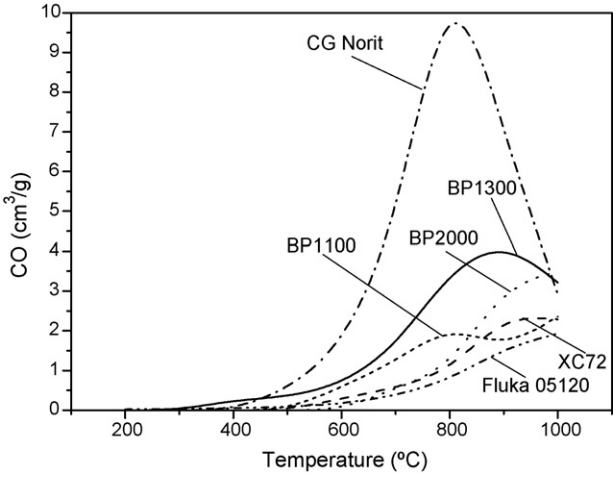


Fig. 6. CO profile obtained by TPD.

which explains the high initial carbon deposition rate. The effect of this group only occurs at the beginning of the run, which also explains the first stage of the curves observed in Fig. 2, in which the carbon deposition rates decay rapidly at the beginning of the tests.

However, as it can be seen from Fig. 5, the presence of oxygenated groups desorbed as $CO_2$ did not affect the initial decomposition rate.

Fig. 6 shows the profiles of the CO desorbed during the TPD runs for each catalyst. It can be observed from the CO profiles that, not only is the amount of OSG different but so is the nature of these groups. It is known that the nature of the surface groups can be determined from the desorbing temperature profile [32,33]. From the analysis of Fig. 6 it can be concluded that the OSG desorbed as CO (at temperatures above 800 °C), plays an important role in methane decomposition. According to the literature [32], these groups could be assigned to quinines and carbonyl groups. A more detailed work is in progress in which the nature of these groups and their evolution during the reaction is being investigated.

### *3.3. Characterization of the catalyst and the deposited carbon*

#### *3.3.1. XRD*

In a previous work, the differences between the XRD spectra of the fresh and deactivated CG Norit catalysts were studied [15]. No substantial difference in the crystallinity of either sample was observed due to the mild contribution of the carbon deposited from methane to the final carbon sample (about 40% of the final carbon sample). It was concluded that the deactivation mechanism could not be associated with differential structural changes. In the present work, the XRD spectra of both fresh and deactivated BP2000 samples are presented. Fig. 7 shows the XRD spectra of both samples. The changes in the crystallinity of the fresh and deactivated samples can be clearly observed. As we have previously mentioned, BP2000 samples can accumulate up to 6 g C/g $C_o$, thus the contribution of the deposited carbon to the final sample weight is 85%. The XRD profiles presented in Fig. 7

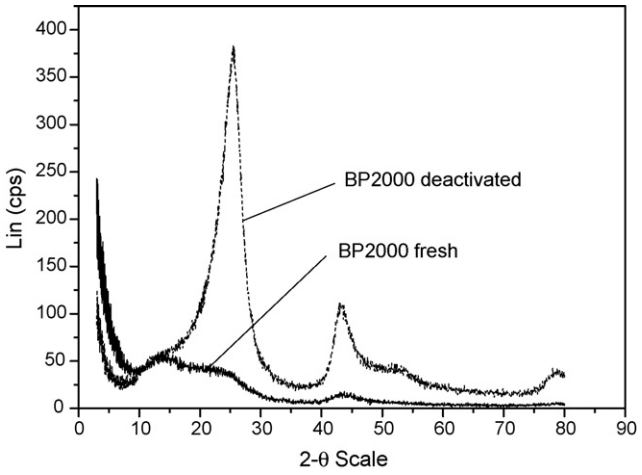


Fig. 7. XRD spectra of the fresh and deactivated BP2000 sample.

show that the fresh BP2000 sample has a disordered structure. However, the deactivated sample presents a more ordered one, which arises from the reflexion present at ∼27° (0 0 2) and at ∼78° (1 0 1), typical of carbons with an ordered structure. This fact can be explained by considering that carbon deposited from methane has a more graphitic structure ($d_{002}$ = 0.3536 nm) than a fresh sample. The presence of huge amount of amorphous carbon in the XRD spectra can be attributed to a carbon material with a turbostratic structure.

In our previous work [14], the most ordered CB samples were less catalytically active when compared to CB with a similar surface area. From the XRD spectra, we can conclude that the more graphitic ordered structure of the deposited carbon does not favour the catalyst activity of the sample.

### 3.3.2. SEM

SEM characterization of the samples was carried out by exploring the surface of the fresh and used carbon catalysts. SEM images of similar samples are available in the literature. However, the external appearance of the samples before and after the TCD run did not change. In the case of BP2000, although the size of primary particles is known to be ca. 15 nm, from the beginning of the reaction 0.5–1 mm spheres are formed by the aggregation of many primary particles. As the run progressed, a gradual increase in the apparent density was observed, ranging from 0.240 g/cm$^3$ for the fresh catalyst to 1.100 g/cm$^3$ for the deactivated carbon catalyst. This indicates that carbon from methane is deposited into the catalyst's particle. To gain knowledge about the possible mechanisms that lead to the catalyst's

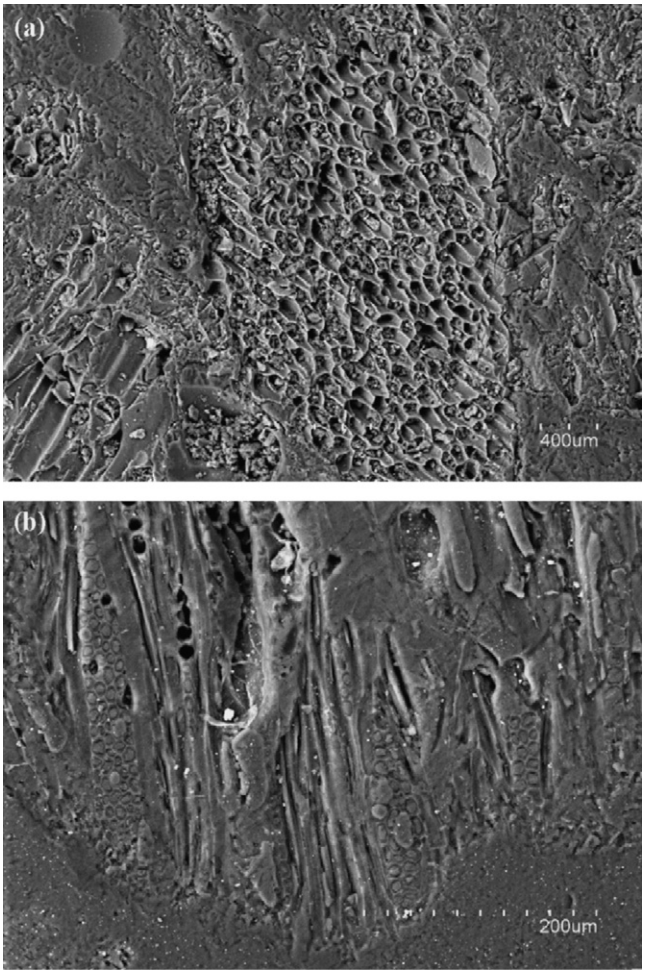


Fig. 8. (a and b) SEM of the fresh and deactivated CG Norit sample.

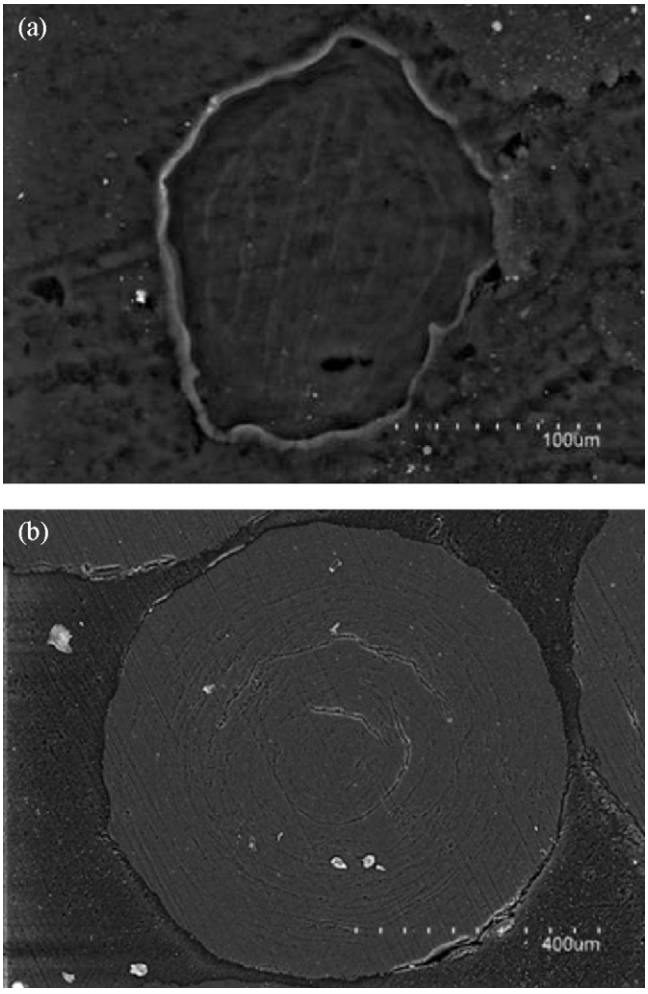


Fig. 9. (a and b) SEM of the fresh and deactivated BP2000 sample.

deactivation, an embedded polymer matrix containing deactivated carbon particles was prepared.

Fig. 8a shows the cross-sectional area of a fresh CG Norit particle. The open macroporosity of the activated carbon can be clearly observed. Fig. 8b shows the cross-sectional area of a deactivated CG Norit particle. It can be observed that most of the open area is occupied by carbon deposits, which provoke the deactivation of the catalyst.

Fig. 9a shows the cross-sectional area of a representative fresh particle of BP2000 carbon black. It has a rounded shape, although it is not completely spherical. The cross-sectional area of the deactivated BP2000 particle is spherical in shape (Fig. 9b), with a diameter ranging from 800 to 1200 μm. It can be observed that the inner volume of the spherical particle is disposed as concentric layers, which look like micro onions.

## 4. Conclusions

The commercial carbon black BP2000 results in the highest amount of carbon deposited, 6.13 g $C_{dep}$/g $C_o$ before deactivation. The highest initial carbon formation rate ($r_o$) among the different samples tested was obtained from the activated carbon CG Norit, (85.9 mg $C_{dep}$/g $C_o$ min). The relationship between the characteristics of the carbonaceous material and its efficiency as a catalyst was also evaluated: the amount of carbon deposited until deactivation shows a linear relationship with the total pore volume of the fresh catalysts and a good correlation is also found between initial reaction rate and the concentration of oxygenated groups desorbed as CO after a TPD experiment.

## Acknowledgements

The authors wish to thank the Spanish MEC (Proyecto ENE2005-03801 Plan Nacional de Energía) for financial support. J.L. Pinilla is in debt with CSIC and Repsol-YPF for the I3P grant.

## References

[1] D. Hart, P. Freud, A. Smith, Hydrogen Today and Tomorrow, IEA GHG Programme, April 1999, ISBN 1 898373248.
[2] $CO_2$ Abatement by the use of Carbon-Rejection Processes, IEA GHG Report PH3/36, February 2001.
[3] M. Steinberg, Int. J. Hydrogen Energy 23 (1998) 419–425.
[4] N.Z. Muradov, Energy Fuels 12 (1998) 41–48.
[5] N.Z. Muradov, T.N. Veziroglu, Int. J. Hydrogen Energy 30 (2005) 225–237.
[6] M.A. Ermakova, D. Yu, A.L. Ermakov, A.L. Chuvilin, G.G. Kuvshinov, J. Catal. 201 (2001) 183–197.
[7] P. Wang, E. Tanabe, K. Ito, J. Jia, H. Morioka, T. Shishido, K. Tahekira, Appl. Catal. A: Gen. 231 (2002) 35–44.
[8] M.A. Ermakova, D. Yu, A.L. Ermakov, G.G. Kuvshinov, Applied Catalysis A: General 201 (2000) 61–70.
[9] Y. Li, J. Chen, Y. Quin, L. Chang, Energy Fuels 14 (2000) 1188–1194.
[10] N. Muradov, Int. J. Hydrogen Energy 26 (2001) 1165–1175.
[11] N. Muradov, Catal. Commun. 2 (2001) 89–94.
[12] M.H. Kim, E.K. Lee, J.H. Jun, G.Y. Han, S.J. Kong, B.K. Lee, T.-J. Lee, K.J. Yoon, Korean J. Chem. Eng. 20 (2003) 835–839.
[13] R. Moliner, I. Suelves, M.J. Lázaro, O. Moreno, Int. J. Hydrogen Energy 30 (2005) 293–300.
[14] I. Suelves, M.J. Lázaro, R. Moliner, J.L. Pinilla, H. Cubero, Int. J. Hydrogen Energy 32 (2007) 3320–3326.
[15] J.L. Pinilla, I. Suelves, R. Utrilla, M.E. Gálvez, M.J. Lázaro, R. Moliner, J of Power Sources 169 (2007) 103–109.
[16] J.L. Pinilla, I. Suelves, M.J. Lázaro, R. Moliner, Chem. Eng. J. (2007), doi:10.1016/j.cej.2007.05.056.
[17] R. Aiello, J.E. Fiscus, H.C. zur Loye, M.D. Amiridis, Appl. Catal. A: Gen. 192 (2000) 227–234.
[18] T. Zhang, M.D. Amiridis, Appl. Catal. A: Gen. 167 (1998) 161–172.
[19] L. Piao, Y. Li, J. Chen, L. Chang, J.Y.S. Lin, Catal. Today 74 (2002) 145–155.
[20] A. Monzón, N. Latorre, T. Ubieto, C. Royo, E. Romeo, J.I. Villacampa, et al., Catal. Today 116 (2006) 264–270.
[21] J.I. Villacampa, C. Royo, E. Romeo, J.A. Montoya, P. del Angel, A. Monzón, Appl. Catal. A: Gen. (2003) 363–383.
[22] M.S. Rahman, E. Croiset, R.R. Hudgins, Topics Catal. 37 (2006) 137–145.
[23] I. Suelves, M.J. Lázaro, R. Molinr, B.M. Corbella, J.M. Palacios, Int. J. Hydrogen Energy 30 (2005) 1555–1567.
[24] F. Rodríguez-Reinoso, Carbon 36 (1998) 159–175.
[25] N.Z. Muradov, Z. Chen, F. Smith, Int. J. Hydrogen Energy 30 (2005) 1149–1158.
[26] E.K. Lee, S.Y. Lee, G.Y. Han, B.K. Lee, T.J. Lee, J.H. Jun, K.J. Yoon, Carbon 42 (2004) 2641–2648.
[27] M.H. Kim, E.K. Lee, J.H. Jun, S.J. Kong, G.Y. Han, T.J. Lee, K.J. Yoon, Int. J. Hydrogen Energy 29 (2004) 89–93.
[28] Z. Bai, H. Chen, B. Li, W. Li, J. Anal. Pyrol. 73 (2005) 3.
[29] V.A. Likholobov, V.B. Fenelonov, L.G. Okkel, O.V. Goncharova, L.B. Avdeeva, V.I. Zaikovskii, G.G. Kuvshinov, React. Kinet. Catal. Lett. 54 (1995) 381–411.
[30] Handbook of Carbon, Graphite, Diamond and Fullerenes, Noyes Publications, 1993.
[31] M.J. Lázaro, M.E. Gálvez, S. Artal, J.M. Palacios, R. Moliner, J. Anal. Pyrol. 78 (2007) 301–315.
[32] J.L. Figueiredo, M.F.R. Pereira, M.M.A. Freitas, J.J.M. Orfão, Carbon 37 (1999) 1379–1389.
[33] G.S. Szymański, Z. Karpiński, S. Biniak, A. Światwoski, Carbon 40 (2002) 2627–2639.